

# Finite temperature QCD crossover at non-zero chemical potential:

## *A Dyson–Schwinger approach*

Arpan Chatterjee,<sup>1</sup> Marco Frasca,<sup>2,\*</sup> Anish Ghoshal,<sup>3,†</sup> and Stefan Groote<sup>1</sup>

<sup>1</sup>*Füüsika Instituut, Tartu Ülikool, W. Ostwaldi 1, EE-50411 Tartu, Estonia*

<sup>2</sup>*Rome, Italy*

<sup>3</sup>*Institute of Theoretical Physics, Faculty of Physics,*

*University of Warsaw, ul. Pasteura 5, 02-093 Warsaw, Poland*

### Abstract

We study QCD at finite temperature and non-zero chemical potential to derive the critical temperature at the chiral phase transition (crossover). We solve a set of Dyson–Schwinger partial differential equations using the exact solution for the Yang–Mills quantum field theory based on elliptical functions. We derive a Nambu–Jona–Lasino (NJL) model of the quarks and obtain a very good agreement with recent lattice computations regarding the dependence of the critical temperature on the strong coupling scale. The solution depends on a single scale parameter, as typical for the theory and already known from studies about asymptotic freedom. The study is analytically derived from QCD.

---

\* marcofrasca@mclink.it

† anish.ghoshal@fuw.edu.pl

## I. INTRODUCTION

Undergoing collisions of large nuclei at the Relativistic Heavy Ion Collider (RHIC) at the Brookhaven National Laboratory (BNL) and the Large Hadron Collider (LHC) create a hot plasma of quarks and gluons with the properties of the early Universe, attaining a very large temperature and involving almost approximate symmetry between matter and antimatter. Future prospects at the FAIR experiment will be able to probe QCD phase diagram structure and to understand the chiral and deconfinement transitions from the hadronic state of matter to the quark-gluon plasma phase. The upcoming devices like the sPHENIX detector, along with foreseen complementary STAR upgrades at RHIC, and together with the plans for the higher luminosity run at the LHC augmented with already present and future upgraded detectors at ALICE, ATLAS, CMS and LHCb, will give us the opportunity to investigate such thermodynamics of QCD with the joint analysis of data from low-energy hadrons, jets, thermal electromagnetic radiation of plasma, heavy quarks, and exotic bound states if they exist [1]. Continuous efforts at the theory frontiers [2–4] along with recent and upcoming plans for state-of-the-art numerical simulations, combined with sophisticated techniques involving machine learning techniques, may be able to give us more promising estimates regarding the uncertainties, in particular the dependence of the uncertainties on the temperature of the plasma. The main difficulty one meets is that, differently from the asymptotic freedom regime, in this energy regions the coupling constant of the strong interactions cannot be used for an application of weak perturbation techniques. Thus, the most relevant approach seems to be lattice computations [5–16]. However, this approach is limited by the sign problem that has a high cost in computational terms [17–20]. This problem implies that regions of higher chemical potential cannot be reached and, presently, it is very difficult to see if the point where a first order phase transition happens for QCD can ever be recovered.

In such a situation, an analytical or semi-analytical approach for QCD at finite temperature and density is strongly needed. On this track, the recent work in Ref. [21] (see also refs. therein) should be pointed out where the authors rely on a minimal model with a numerical solution of the set of Dyson–Schwinger equations. They are able to obtain

good agreement with lattice data for the critical temperature at finite chemical potential. It should be pointed out that lattice computations work for a small ratio  $\mu_B/T_c(0)$ , evaluating the dependence of  $T_c(\mu_B)$  on the chemical potential through a Taylor series. In the range explored so far, lattice computations do not show any phase transition point beyond the chiral crossover.

If a critical end point (CEP) exists in the QCD phase diagram and one is able to understand the regions of the parameter space involving the chemical potential allowing for a first-order phase transition, the knowledge of crossovers will be important milestones for such an experimental endeavour.

Non-perturbative methods are mandatory in this endeavour. Although lattice QCD investigations have shown the analytic crossover at zero chemical potential [6, 7, 22–25], the result suffers from the infamous fermion sign problem in presence of any (real) chemical potential. This sign problem means that one has a high cost in computational terms [17–20]. In literature, a myriad of methods concerning the extrapolation from zero or imaginary chemical potential into the real chemical potential region are exploited, and usually they agree with each other for chemical potentials  $\mu_B/T < 2$ . However, these too suffer from errors for larger chemical potential, with the consequence of concrete predictions still eluding.

One of possible ways to capture the effect of large chemical potential is what is known as the continuum methods, i.e., effective field theory models and the functional approach. For instance, the Polyakov-loop enhanced effective models like the Polyakov-loop Nambu–Jona–Lasinio model (PNJL) as proposed in Refs. [26–28], or the Polyakov-loop quark-meson model (PQM) [29–31], have been investigated to explore various aspects of the QCD phase diagram, see e.g. [32, 33] for recent review articles on this topic. Essentially, these methods rely on a simple chiral effective action which is then added to the Polyakov loop potential. Such an action, serving as a background that couples to Yang–Mills interactions, leads in particular to confinement properties of the chiral dynamics. But as understood in this manner, the effect of the presence of gluons in the medium cannot be captured, as they are not directly active degrees of freedom. This becomes possible within functional approaches to QCD. In particular, Dyson–Schwinger equations (DSE), the functional renormalisation group, the Hamilton variational approach, and the Gribov–Zwanziger formalism are some

example scenarios where one works with the quark and gluon degrees of freedom. In this manner one is able to understand somewhat the phase structure of QCD from the order parameter point of view, mainly extracted directly from Green's functions of the theory. For the past several years, these methods involving functionals were able to give us somewhat a preliminary picture of the QCD phase diagram along with some characteristic properties of quarks and gluons in the plasma. With such insights they were influential in understanding the implications of observables related to QCD thermodynamics, the complex nature of the transport, and fluctuations of QCD in the framework of DSE and Bethe–Salpeter equations, see the reviews by Roberts and Schmidt [34] and Fisher [35].

Our aim in this work is to show how a fully analytical approach can be derived from QCD and implemented to evaluate the critical temperature as a function of the chemical potential. We use an exact solution to the gluonic sector of QCD recently obtained in Ref. [36]. This solution exploits the fact that the vacuum as a Fubini–Lipatov instanton could break translation invariance [37, 38]. However, such a violation could never be observed, as the Yang–Mills field and its potentials are never observable and the propagator recovers such a symmetry. We already applied this idea successfully to the evaluation of the hadron vacuum polarisation contribution to the  $g - 2$  of the muon [39], and our result still stands against the most recent evaluations of this quantity by lattice computations [40, 41] and the experimental data [42, 43]. Based on the same background, we present a derivation of the critical temperature  $T_c(\mu_B)$  by analytical means, and we show good agreement with lattice data, in the given range of the chemical potential, by using a single parameter that is an energy scale already characterizing QCD in the regime of asymptotic freedom.

The paper is structured in two main sections: In order to make the paper self-contained, in Sec. II we give a derivation from QCD in the infrared limit. In Sec. III, we introduce temperature and chemical potential and compare our result for the critical temperature with lattice data. In Sec. IV, our conclusions are presented.

## II. QCD IN THE INFRARED LIMIT

For the sake of completeness, in this section we briefly summarize the derivation of a non-local Nambu–Jona-Lasinio model. Details are presented elsewhere [44–47]. Compared to the previous analysis, we improve on the form of the propagator in agreement with the existence of exact solutions of the massless scalar field [48].

Starting point for the derivation is the QCD lagrangian

$$\mathcal{L}_{\text{QCD}} = \sum_i \bar{\psi}^i (i\gamma^\mu D_\mu - m_i) \psi^i - \frac{1}{4} F_{\mu\nu}^a F_a^{\mu\nu} - \frac{1}{2\xi} (\partial_\mu A_\mu^a)^2. \quad (1)$$

Here  $A$  represents the gluon field and  $\psi$  the QCD quarks,  $m$  is the mass and  $i$  are the various flavours of the quark.  $\xi$  is the gauge fixing parameter. The gluon field is coupled minimally via the covariant derivative  $D_\mu = \partial_\mu + ig_s A_\mu^a T_a$ , and the field strength tensor  $F_{\mu\nu} = F_{\mu\nu}^a T_a$  is given by  $ig_s F_{\mu\nu} = [D_\mu, D_\nu]$ , so that  $F_{\mu\nu}^a(x) = \partial_\mu A_\nu^a(x) - \partial_\nu A_\mu^a(x) - g_s f_{abc} A_\mu^b(x) A_\nu^c(x)$ . Written explicitly, the action integral reads

$$\begin{aligned} \mathcal{S}_{\text{QCD}} = \int d^4x \left[ \sum_i \bar{\psi}^i(x) (i\gamma^\mu \partial_\mu - m_i - g_s \gamma^\mu A_\mu^a(x) T_a) \psi^i(x) + \right. \\ \left. + \frac{1}{2} A_\mu^a(x) (\eta^{\mu\nu} \square - \partial^\mu \partial^\nu) A_\nu^a(x) + \frac{1}{2\xi} A_\mu^a(x) \partial^\mu \partial^\nu A_\nu^a(x) + \right. \\ \left. + \frac{1}{2} g_s f_{abc} (\partial_\mu A_\nu^a(x) - \partial_\nu A_\mu^a(x)) A_b^\mu(x) A_c^\nu(x) - \frac{1}{4} g_s^2 f_{abc} f_{cde} A_a^\mu(x) A_b^\nu(x) A_\mu^d(x) A_\nu^e(x) \right]. \quad (2) \end{aligned}$$

The Euler–Lagrange equations for the gluon fields are given by

$$\begin{aligned} 0 = \frac{\delta \mathcal{S}_{\text{QCD}}}{\delta A_\mu^a} = (\square \eta^{\mu\nu} - \partial^\mu \partial^\nu) A_\nu^a + \frac{1}{\xi} \partial^\mu \partial^\nu A_\nu^a - j_a^\mu + \\ + g_s f_{abc} \partial_\nu A_b^\mu A_c^\nu + g_s f_{abc} A_\nu^b (\partial^\mu A_c^\nu - \partial^\nu A_c^\mu) - g_s^2 f_{abc} f_{cde} A_\nu^b A_d^\mu A_e^\nu, \quad (3) \end{aligned}$$

where we use  $j_a^\mu = g_s \bar{\psi} \gamma^\mu T_a \psi$  to replace the fermionic current by a generic one.  $T_a$  are the Gell-Mann matrices. Feynman gauge  $\xi = 1$  is employed to simplify the equation of motion.

### A. Solving the system of Dyson–Schwinger equations

The Euler–Lagrange equation can be translated to an equation of motion for the Green functions, constructed from the generating functional  $Z[j]$ , from which the system of Dyson–Schwinger equations is derived. We start with  $\langle A_\mu^a(x) \rangle = Z[j] G_{1\mu}^{(j)a}(x)$ , and by calculating

the functional derivative with respect to  $j_b^\nu(x')$ , we continue with

$$\langle A_\mu^a(x)A_\nu^b(x') \rangle = Z[j]G_{2\mu\nu}^{(j)ab}(x, x') + Z[j]G_{1\mu}^{(j)a}(x)G_{1\nu}^{(j)b}(x'). \quad (4)$$

Finally, a further functional derivative with respect to  $j_\nu^b(x'')$  and the setting  $x = x' = x''$  lead to

$$\begin{aligned} \langle A_b^\nu(x)A_\mu^d(x)A_\nu^e(x) \rangle &= Z[j] \left( G_{3\mu\nu b}^{(j)de\nu}(x, x, x) + G_{2\mu b}^{(j)d\nu}(x, x)G_{1\nu}^{(j)e}(x) + \right. \\ &\quad \left. + G_{1\mu}^{(j)d}(x)G_{2\nu b}^{(j)e\nu}(x, x) + G_{1b}^{(j)\nu}(x)G_{2\mu\nu}^{(j)de}(x, x) + G_{1b}^{(j)\nu}(x)G_{1\mu}^{(j)d}(x)G_{1\nu}^{(j)e}(x) \right). \end{aligned} \quad (5)$$

Inserting all this into the expectation value of the Euler–Lagrange equation results in

$$\begin{aligned} \square G_{1\mu}^{(j)a}(x) - j_\mu^a(x) &= g_s f_{abc} \left\{ \partial^\nu \left( G_{2\mu\nu}^{(j)bc}(x, x) + G_{1\mu}^{(j)b}(x)G_{1\nu}^{(j)c}(x) \right) + \right. \\ &\quad \left. + \left( \partial_\mu G_{2\nu b}^{(j)c\nu}(x, x) - \partial_\nu G_{2\mu b}^{(j)c\nu}(x, x) \right) + G_{1b}^{(j)\nu}(x) \left( \partial_\mu G_{1\nu}^{(j)c}(x) - \partial_\nu G_{1\mu}^{(j)c}(x) \right) \right\} + \\ &\quad - g_s^2 f_{abc} f_{cde} \left\{ G_{3\mu\nu b}^{(j)de\nu}(x, x, x) + G_{2\mu b}^{(j)d\nu}(x, x)G_{1\nu}^{(j)e}(x) + \right. \\ &\quad \left. + G_{1\mu}^{(j)d}(x)G_{2\nu b}^{(j)e\nu}(x, x) + G_{1b}^{(j)\nu}(x)G_{2\mu\nu}^{(j)de}(x, x) + G_{1b}^{(j)\nu}(x)G_{1\mu}^{(j)d}(x)G_{1\nu}^{(j)e}(x) \right\}. \end{aligned} \quad (6)$$

Next we calculate the functional derivative with respect to  $j_h^\lambda(y)$  to obtain

$$\begin{aligned} \square G_{2\mu\lambda}^{(j)ah}(x, y) + i\delta^{ah}\eta_{\mu\lambda}\delta^{(4)}(x-y) &= g_s f_{abc} \left\{ \left( \partial_\mu G_{3\nu b\lambda}^{(j)cvh}(x, x, y) - \partial_\nu G_{3\mu b\lambda}^{(j)cvh}(x, x, y) \right) + \right. \\ &\quad \left. + \partial^\nu \left( G_{3\mu\nu\lambda}^{(j)bch}(x, x, y) + G_{2\mu\lambda}^{(j)bh}(x, y)G_{1\nu}^{(j)c}(x) + G_{1\mu}^{(j)b}(x)G_{2\nu\lambda}^{(j)ch}(x, y) \right) + \right. \\ &\quad \left. + G_{2b\lambda}^{(j)\nu h}(x, y) \left( \partial_\mu G_{1\nu}^{(j)c}(x) - \partial_\nu G_{1\mu}^{(j)c}(x) \right) + G_{1b}^{(j)\nu}(x) \left( \partial_\mu G_{2\nu\lambda}^{(j)ch}(x, y) - \partial_\nu G_{2\mu\lambda}^{(j)ch}(x, y) \right) \right\} + \\ &\quad - g_s^2 f_{abc} f_{cde} \left\{ \left( G_{4\mu\nu b\lambda}^{(j)de\nu h}(x, x, x, y) + G_{3\mu\nu b}^{(j)d\nu h}(x, x, y)G_{1\nu}^{(j)e}(x) + G_{2\mu b}^{(j)d\nu}(x, x)G_{2\nu\lambda}^{(j)eh}(x, y) + \right. \right. \\ &\quad \left. + G_{2\mu\lambda}^{(j)dh}(x, y)G_{2\nu b}^{(j)e\nu}(x, x) + G_{1\mu}^{(j)d}(x)G_{3\nu b\lambda}^{(j)e\nu h}(x, x, y) \right) + \\ &\quad \left. + G_{2b\lambda}^{(j)\nu h}(x, y) \left( G_{2\mu\nu}^{(j)de}(x, x) + G_{1\mu}^{(j)d}(x)G_{1\nu}^{(j)e}(x) \right) + \right. \\ &\quad \left. + G_{1b}^{(j)\nu}(x) \left( G_{3\mu\nu\lambda}^{(j)deh}(x, x, y) + G_{2\mu\lambda}^{(j)dh}(x, y)G_{1\nu}^{(j)e}(x) + G_{1\mu}^{(j)d}(x)G_{2\nu\lambda}^{(j)eh}(x, y) \right) \right\}. \end{aligned} \quad (7)$$

Using the mapping theorem for Yang–Mills [49, 50] with  $G_{\mu\nu}^{(2)ab}(x, y) = \delta_{ab}\eta_{\mu\nu}G_2(x-y)$ ,  $G_\mu^{(1)a}(x) = \eta_\mu^a G_1(x)$  and  $j_a^\mu(x) = \eta_a^\mu j(x)$  and contracting with bases dual with respect to the orthogonality and completeness relations

$$\eta_\mu^a \eta_b^\mu = -\delta_b^a, \quad \eta_\mu^a \eta_\nu^a = -(N_c^2 - 1)\eta_{\mu\nu}/D, \quad (8)$$

leads to the scalar equations

$$\square G_1(x) + N_c g_s^2 \left\{ (D-1)G_2(0)G_1(x) + G_1(x)^3 \right\} = j(x), \quad (9)$$

$$\square G_2(x-y) + (D-1)N_c g_s^2 (G_2(0) + G_1(x)^2) G_2(x-y) = -i\delta^{(4)}(x-y). \quad (10)$$

where  $D$  is the space-time dimension. For  $\Delta m_G^2 := (D-1)\lambda G_2(0)$  with  $\lambda := N_c g_s^2$ , where  $N_c$  is the number of colour charges, the equation of motion for the one-point function  $G_1(x)$  reduces to  $(\square + \Delta m_G^2)G_1(x) + \lambda G_1(x)^3 = j(x)$ . In the following we can choose  $D = 4$ . The corresponding homogeneous equation is solved by

$$G_1(x) = \mu \operatorname{sn}(k \cdot x + \theta | \kappa) = -i\mu\eta \sum_{m \text{ odd}} \sqrt{\kappa} b_m e^{im\eta kx/2}, \quad b_{2n+1} := \frac{(-1)^n q^{n+1/2}}{\sqrt{\kappa}(1-q^{2n+1})}, \quad (11)$$

where  $\kappa := (\Delta m_G^2 - k^2)/k^2$ ,  $q := \exp(-\pi K(1-\kappa)/K(\kappa))$  and  $\eta := \pi/K(\kappa)$  ( $K(\kappa)$  is the complete elliptic integral of the first kind), with the dispersion relation given by

$$k^2 = \Delta m_G^2 + \frac{1}{2}\lambda\mu^2. \quad (12)$$

$\mu$  and  $\theta$  are integration constants, where  $\theta = (1+4N)K(\kappa)$  for an arbitrary integer  $N$  is fixed in turn by solving the equation  $(\square + \Delta m_G^2 + 3\lambda G_1(x)^2)G_2(x-y) = \delta^{(4)}(x-y)$  for the two-point function.

$$K(\kappa) = F(\pi/2|\kappa), \quad \text{with } F(\varphi|\kappa) = \int_0^\varphi \frac{d\theta}{\sqrt{1-\kappa \sin^2 \theta}} \quad (13)$$

is the complete elliptic integral of the first kind, and  $\operatorname{sn}(z|\kappa) = \sin \varphi$  is the corresponding Jacobi elliptic sine, solution of  $z = F(\varphi|\kappa)$ . For the two-point Green function one ends up with the momentum space expression

$$\tilde{G}_2(p) = \sum_{n=0}^{\infty} \frac{iB_n}{p^2 - m_n^2 + i\epsilon}, \quad B_n := \frac{(2n+1)^2 \eta^3}{2(1-\kappa)} b_{2n+1}, \quad (14)$$

with  $m_n := (2n+1)m_0$  and  $m_0 = \eta\sqrt{k^2}/2$ , where in addition we found that  $\sum_{n=0}^{\infty} B_n = 1$ .

Finally, we arrive at

$$G_2(x-y) = \sum_{n=0}^{\infty} \int \frac{d^4 p}{(2\pi)^4} \frac{iB_n e^{-ip(x-y)}}{p^2 - m_n^2 + i\epsilon}. \quad (15)$$

Using this Green function, the general solution of the inhomogeneous equation (9) reads

$$\phi(x) = G_1(x) + \int G_2(x-y)j(y)dy. \quad (16)$$

Note that for the nonlinear differential equation at hand, this holds only approximately, where the expansion parameter of the approximation is given by the charge  $g_s$  related to the current  $j(x)$ . Therefore, higher functional powers of  $j$  can be omitted safely.

## B. Deriving the non-local Nambu–Jona-Lasinio model

Returning to the original Lagrange density, the inhomogeneous equation to be solved is of the shape

$$\square A_a^\nu(x) + \dots = g_s \sum_i \bar{\psi}^i(x) \gamma^\nu T_a \psi^i(x). \quad (17)$$

The stationary solution is obtained by convolution with the Green function,

$$A_a^\nu(x) = -ig_s \int G_2(x-y) \sum_j \bar{\psi}^j(y) \gamma^\nu T_a \psi^j(y) d^4y, \quad (18)$$

which again can be inserted into the equation of motion for the quark field to give

$$0 = \frac{\partial \mathcal{L}}{\partial \bar{\psi}^i} - \partial_\mu \frac{\partial \mathcal{L}}{\partial (\partial_\mu \bar{\psi}^i)} = \frac{\partial \mathcal{L}}{\partial \bar{\psi}^i} = (i\gamma^\mu \partial_\mu - m_i - g_s \gamma^\mu A_\mu^a T_a) \psi^i. \quad (19)$$

Inserting the stationary solution for the Yang–Mills field one obtains

$$0 = (i\gamma^\mu \partial_\mu - m_i) \psi^i(x) - ig_s^2 \gamma^\mu T_a \psi^i(x) \int \sum_j G_2(x-y) \bar{\psi}^j(y) \gamma_\mu T_a \psi^j(y) d^4y, \quad (20)$$

from which one derives the action integral of the quark flavour dynamics (QFD) to be

$$\begin{aligned} \mathcal{S}_{\text{QFD}} = & \int \sum_i \bar{\psi}^i(x) (i\gamma^\mu \partial_\mu - m_i) \psi^i(x) d^4x + \\ & - ig_s^2 \int \sum_{i,j} \bar{\psi}^i(x) \gamma^\mu T_a \psi^i(x) G_2(x-y) \bar{\psi}^j(y) \gamma_\mu T_a \psi^j(y) d^4y d^4x. \end{aligned} \quad (21)$$

The currents occurring in the interaction part are coloured. In order to obtain a Nambu–Jona–Lasinio (NJL) action that describes the interaction between colourless mesons, we have to perform a Fierz rearrangement. This is a rearrangement in both the colour and spinor

states and reads [51–53]

$$\begin{aligned}
& g_s^2 \bar{\psi}^i(x) \gamma^\mu T_a \psi^i(x) \bar{\psi}^j(y) \gamma_\mu T^a \psi^j(y) = \\
& = \frac{N_c^2 - 1}{2N_c^2} g_s^2 \left( \bar{\psi}^i(x) \psi^j(y) \bar{\psi}^j(y) \psi^i(x) + \bar{\psi}^i(x) i\gamma_5 \psi^j(y) \bar{\psi}^j(y) i\gamma_5 \psi^i(x) + \right. \\
& \quad \left. - \frac{1}{2} \bar{\psi}^i(x) \gamma_\mu \psi^j(y) \bar{\psi}^j(y) \gamma^\mu \psi^i(x) - \frac{1}{2} \bar{\psi}^i(x) \gamma_5 \gamma_\mu \psi^j(y) \bar{\psi}^j(y) \gamma_5 \gamma^\mu \psi^i(x) \right) + \\
& \quad - \frac{g_s^2}{N_c} \left( \bar{\psi}^i(x) T_a \psi^j(y) \bar{\psi}^j(y) T_a \psi^i(x) - \bar{\psi}^i(x) \gamma_5 T_a \psi^j(y) \bar{\psi}^j(y) \gamma_5 T_a \psi^i(x) + \right. \\
& \quad \left. - \frac{1}{2} \bar{\psi}^i(x) \gamma_\mu T_a \psi^j(y) \bar{\psi}^j(y) \gamma^\mu T_a \psi^i(x) - \frac{1}{2} \bar{\psi}^i(x) \gamma_5 \gamma_\mu T_a \psi^j(y) \bar{\psi}^j(y) \gamma_5 \gamma^\mu T_a \psi^i(x) \right).
\end{aligned} \tag{22}$$

The result consists of a singlet and an octet contribution. Because of the minus sign, the latter is repulsive and will not contribute to a meson bound state. In addition, the limit  $N_c \rightarrow \infty$  will make it vanish. Therefore, we keep only this first part that again contains scalar, pseudoscalar, vector, and axial vector currents. As the (two) flavour states are now mixed, we can divide  $\bar{\psi}^i(x) \psi^j(y)$  up into the isoscalar current  $\bar{\psi}^i(x) \delta_{ij} \psi^j(y)$  and the isovector current  $\bar{\psi}^i(x) \vec{\sigma}_{ij} \psi^j(y)$  where  $\vec{\sigma} = (\sigma_1, \sigma_2, \sigma_3) \in SU(2)_f$ . Finally, we take out the scalar–isoscalar and the pseudoscalar–isovector currents as those representing physical mesons, and combine them into a four-vector current  $\bar{\psi}(x) \Gamma^\alpha \psi(y)$  (employing  $\Gamma^0 = \mathbb{1}$  and  $\Gamma^i = \gamma_5 \sigma_i = -\Gamma_i$ ) with  $\bar{\psi}(y) \Gamma^\alpha \psi(x) = (\bar{\psi}(x) \Gamma^\alpha \psi(y))^*$  to obtain

$$\begin{aligned}
\mathcal{S}_{\text{NJL}} & = \int \bar{\psi}(x) (i\gamma^\mu \partial_\mu - \hat{m}) \psi(x) d^4x + \\
& \quad - i \frac{N_c^2 - 1}{2N_c^2} g_s^2 \int \bar{\psi}(x) \Gamma_\alpha \psi(y) G_2(x-y) \bar{\psi}(y) \Gamma^\alpha \psi(x) d^4y d^4x,
\end{aligned} \tag{23}$$

where  $\hat{m} = \text{diag}\{m_i\}$  is the constituent quark mass matrix in flavour space. Using the relative coordinates  $w = (x+y)/2$  and  $z = x-y$  ( $x = w+z/2$ ,  $y = w-z/2$ ), one replaces the two-point Green function by  $G_2(z) = -iG\mathcal{C}(z)/2$  with  $G = 2/((1-\kappa)k^2)$ . It is easy to show that  $\tilde{\mathcal{C}}(0) = \int \mathcal{C}(z) d^4z = 1$ , a detail that is postponed to Appendix A.

### C. Performing the bosonisation procedure

For the interaction part of the NJL action, one obtains [54]

$$\mathcal{S}_{\text{int}} = -\frac{GG_S^2}{2} \int \bar{\psi}(w + \frac{z}{2}) \Gamma_\alpha \psi(w - \frac{z}{2}) \mathcal{C}(z) \bar{\psi}(w - \frac{z}{2}) \Gamma^\alpha \psi(w + \frac{z}{2}) d^4w d^4z \tag{24}$$

with  $G_S^2 := (N_c^2 - 1)g_s^2/(2N_c^2)$ . Including  $\mathcal{S}_0 = \int \bar{\psi}(x)(i\gamma^\mu \partial_\mu - \hat{m})\psi(x)d^4x$ , the functional integral reads  $\mathcal{Z}_{\text{NJL}} = \int \mathcal{D}\bar{\psi}\mathcal{D}\psi \exp(i(\mathcal{S}_0 + \mathcal{S}_{\text{int}}))$ . In order to perform the bosonisation, one adds a mesonic field  $(\phi^\alpha) = (\sigma, \vec{\pi})$  by multiplying the factor

$$\mathcal{N}^{-1} = \int \mathcal{D}\phi^* \mathcal{D}\phi \exp\left(\frac{-i}{2G} \int \mathcal{C}(z)\phi_\alpha^*(w)\phi^\alpha(w)d^4w d^4z\right), \quad (25)$$

to the functional integral, leading to an action  $\mathcal{S}_{\text{int}+}$ . Note that the integration over  $z$  is actually trivial. Still, one needs this integration to perform the functional shift

$$\phi_\alpha(w) \rightarrow \phi_\alpha(w) - GG_S \bar{\psi}(w - \frac{z}{2})\Gamma_\alpha \psi(w + \frac{z}{2}). \quad (26)$$

In performing this shift, the quartic interaction cancels and one obtains the action integral

$$\begin{aligned} \mathcal{S}_{\text{int}+}[\psi, \bar{\psi}, \phi, \phi^*] &= \int \left[ \frac{1}{2G} \mathcal{C}(z)\phi_\alpha^*(w)\phi^\alpha(w) + \right. \\ &\quad \left. - \frac{G_S \mathcal{C}(z)}{2} \left( \phi_\alpha(w)\bar{\psi}(w + \frac{z}{2})\Gamma^\alpha \psi(w - \frac{z}{2}) + \phi_\alpha^*(w)\psi(w - \frac{z}{2})\Gamma^\alpha \psi(w + \frac{z}{2}) \right) \right] d^4w d^4z = \\ &= \frac{1}{2G} \int \phi_\alpha^*(w)\phi^\alpha(w)d^4w - G_S \int \bar{\psi}(x)\mathcal{C}(x-y) \text{Re} \phi_\alpha\left(\frac{x+y}{2}\right) \Gamma^\alpha \psi(y)d^4x d^4y, \end{aligned} \quad (27)$$

where one has returned to the previous coordinates, though for the second term in reverse order (note that  $\mathcal{C}(x-y) = \mathcal{C}(y-x)$ ). The main bosonisation process consists in integrating out the fermionic fields. This is done by performing a Fourier transform to

$$\begin{aligned} \mathcal{S}_{\text{int}+}[\psi, \bar{\psi}, \phi, \phi^*] &= \frac{1}{2G} \int \frac{d^4q}{(2\pi)^4} \tilde{\phi}_\alpha^*(q)\tilde{\phi}^\alpha(q) + \\ &\quad - \frac{G_S}{2} \int \frac{d^4p'}{(2\pi)^4} \frac{d^4p}{(2\pi)^4} \tilde{\psi}(p')\tilde{\mathcal{C}}\left(\frac{p'+p}{2}\right) \left( \tilde{\phi}_\alpha(p'-p) + \tilde{\phi}_\alpha(p-p') \right) \Gamma^\alpha \tilde{\psi}(p), \end{aligned} \quad (28)$$

combining  $\mathcal{S}_0$  with the second part of  $\mathcal{S}_{\text{int}+}$ , and performing the calculation

$$\begin{aligned} &\int \mathcal{D}\bar{\psi}\mathcal{D}\psi \exp \left[ i \int \frac{d^4p'}{(2\pi)^4} \frac{d^4p}{(2\pi)^4} \tilde{\psi}(p') \times \right. \\ &\quad \times \left( (2\pi)^4 \delta^{(4)}(p'-p)(\gamma^\mu p_\mu - \hat{m}) - \frac{G_S}{2} \tilde{\mathcal{C}}\left(\frac{p'+p}{2}\right) \left( \tilde{\phi}_\alpha(p'-p) + \tilde{\phi}_\alpha(p-p') \right) \Gamma^\alpha \right) \tilde{\psi}(p) \left. \right] = \\ &= \det \left( (2\pi)^4 \delta^{(4)}(p'-p)(\gamma^\mu p_\mu - \hat{m}) - \frac{G_S}{2} \tilde{\mathcal{C}}\left(\frac{p'+p}{2}\right) \left( \tilde{\phi}_\alpha(p'-p) + \tilde{\phi}_\alpha(p-p') \right) \Gamma^\alpha \right). \end{aligned} \quad (29)$$

The matrix of which the determinant is taken is understood as being expressed not only in terms of Dirac and (trivial) colour and flavour matrices but also between states  $|p\rangle$  and  $|p'\rangle$ .

The bosonisation procedure is completed by the mean field approximation  $\phi(z) = (\bar{\sigma}, \vec{0})$ , resulting in  $\phi_\alpha(p' - p) = (2\pi)^4 \delta^{(4)}(p' - p) \bar{\sigma} \delta_{\alpha 0}$ . This renders the trace over states a single four-dimensional integration. For the determinant one obtains

$$\det \left( (2\pi)^4 \delta^{(4)}(p' - p) (\gamma^\mu p_\mu - \hat{M}_f(p)) \right) = \int \frac{d^4 p}{(2\pi)^4} \prod_f (p^2 - M_f^2(p))^{2N_c}, \quad (30)$$

where  $\hat{M}_f(p) = \hat{m}_f + G_S \tilde{\mathcal{C}}(p) \bar{\sigma} \mathbb{1}$  is the gap mass matrix in flavour space with diagonal elements  $M_f(p) = m_f + G_S \tilde{\mathcal{C}}(p) \bar{\sigma}$ . Therefore, the bosonised action integral is given by

$$\mathcal{S}_{\text{bos}} = \frac{\bar{\sigma}^2}{2G} - 2iN_c \int \frac{d^4 p}{(2\pi)^4} \sum_f \ln(p^2 - M_f^2(p)), \quad (31)$$

In calculating the variation with respect to  $\bar{\sigma}$  one obtains

$$\bar{\sigma} = -4iN_c G G_S \int \frac{d^4 p}{(2\pi)^4} \sum_f \frac{\tilde{\mathcal{C}}(p) M_f(p)}{p^2 - M_f^2(p)}, \quad (32)$$

and inserting this into the formula for  $M_f(p)$ , one ends up with the mass gap equation

$$M_q(p) = m_q - 4iN_c G G_S^2 \tilde{\mathcal{C}}(p) \int \frac{d^4 q}{(2\pi)^4} \sum_f \frac{\tilde{\mathcal{C}}(q) M_f(q)}{q^2 - M_f^2(q)}. \quad (33)$$

For massless quarks, the sum over the flavours is performed trivially and results in

$$M(p) = -4iN_f N_c G G_S^2 \tilde{\mathcal{C}}(p) \int \frac{d^4 q}{(2\pi)^4} \frac{\tilde{\mathcal{C}}(q) M(q)}{q^2 - M^2(q)}. \quad (34)$$

### III. QCD AT FINITE TEMPERATURE

#### A. Introducing the temperature

In the following, we deal with massless quarks. At finite temperature, the integration over the zeroth momentum component is replaced by a Matsubara sum, resulting in

$$M(i\omega_k, \vec{p}) = 4N_f N_c G G_S^2 \tilde{\mathcal{C}}(i\omega_k, \vec{p}) \beta^{-1} \sum_{l=-\infty}^{\infty} \int \frac{d^3 q}{(2\pi)^3} \frac{\tilde{\mathcal{C}}(i\omega_l, \vec{q}) M(i\omega_l, \vec{q})}{\omega_l^2 + \vec{q}^2 + M^2(i\omega_l, \vec{q})}. \quad (35)$$

Using  $M(i\omega_k, \vec{p}) = \tilde{\mathcal{C}}(i\omega_k, \vec{p}) G_S \bar{\sigma}$ , the mass gap equation can be rewritten into a mass gap equation for  $\bar{\sigma}$ ,

$$1 = 4N_f N_c G G_S^2 \beta^{-1} \sum_{k=-\infty}^{+\infty} \int \frac{d^3 p}{(2\pi)^3} \frac{\tilde{\mathcal{C}}^2(i\omega_k, \vec{p})}{\omega_k^2 + \vec{p}^2 + \tilde{\mathcal{C}}^2(i\omega_k, \vec{p}) G_S^2 \bar{\sigma}^2} =: f_M(\beta^{-1}). \quad (36)$$

Using  $N_f = 3$ ,  $N_c = 3$ ,  $\omega_k = (2k + 1)\omega_0$ ,  $\omega_0 = \pi/\beta$ ,

$$G = \frac{2}{(1 - \kappa)k^2} = \frac{2K(\kappa)^2}{(1 - \kappa)\pi^2 m_0^2}, \quad G_S^2 = \frac{N_c^2 - 1}{2N_c^2} g_s^2 = \frac{4}{9} 4\pi\alpha_s \quad (37)$$

(note that for  $\kappa = -1$ ,  $G$  is equal to the inverse string tension), and

$$\tilde{C}(i\omega_k, \vec{p}) = \sum_{n=0}^{\infty} \frac{m_0^2 C_{2n+1}(\kappa)}{\omega_k^2 + \vec{p}^2 + (2n+1)^2 m_0^2}, \quad C_\nu(\kappa) = \frac{2\pi\nu^2}{K(\kappa)} \frac{(-1)^n q^{\nu/2}}{\sqrt{\kappa}(1 - q^\nu)} = C_{-\nu}(\kappa) \quad (38)$$

with nome  $q = \exp(-\pi K(1 - \kappa)/K(\kappa))$  (again for  $\kappa = -1$ , one has  $q = \exp(-(1 - i)\pi)$  and, therefore,  $C_\nu(-1) = (2\pi\nu^2/K(-1))e^{\pi\nu/2}/(1 + e^{\pi\nu}) = C_{-\nu}(-1)$ ).

Eq. (36) can be rendered as a dimensionless equation by using  $\hat{m}_0 = \beta m_0/2$ ,  $\hat{\omega}_0 = \beta\omega_0/2 = \pi/2$  and  $\hat{\rho} = \beta\rho/2$ . As such, the equation is no longer dependent on the temperature and on the ground state Matsubara frequency. The mass gap equation reads

$$1 = \frac{N_f N_c \hat{G} G_S^2}{\pi^2} \sum_{k=-\infty}^{+\infty} \int_0^\infty \frac{\tilde{C}^2(i\hat{\omega}_k, \hat{\rho}) \hat{\rho}^2 d\hat{\rho}}{\hat{\omega}_k^2 + \hat{\rho}^2 + \tilde{C}^2(i\hat{\omega}_k, \hat{\rho}) \hat{\sigma}^2}. \quad (39)$$

with  $\hat{\sigma} := \beta G_S \bar{\sigma}/2$ ,

$$\hat{\omega}_k = (2k + 1)\hat{\omega}_0 = \frac{1}{2}(2k + 1)\pi, \quad \hat{G} = \frac{2K(\kappa)^2}{(1 - \kappa)\pi^2 \hat{m}_0^2} = \frac{4G}{\beta^2}. \quad (40)$$

## B. Including the quark chemical potential

Now we can include the quark chemical potential  $\mu_f$ . For this we start with the grand canonical potential

$$\Omega = -\frac{1}{2\beta} \sum_{k=-\infty}^{+\infty} \int \frac{d^3p}{(2\pi)^3} \text{Tr} \ln \left[ \beta \tilde{S}^{-1}(i\omega_k; \vec{p}) \right] + \frac{\bar{\sigma}^2}{2G} \quad (41)$$

with an additional factor 1/2 because of the doubling of the degrees of freedom in the inverse Nambu–Gor’kov propagator

$$\tilde{S}^{-1}(i\omega_k; \vec{p}) = \begin{pmatrix} ((i\omega_k \mathbb{1}_c - A_4) \mathbb{1}_f + \hat{\mu}_f \mathbb{1}_c) \gamma^0 - \vec{\gamma} \cdot \vec{p} \mathbb{1}_{c,f} - \hat{M}(i\omega_k, \vec{p}) \mathbb{1}_d & 0 \\ 0 & ((i\omega_k^* \mathbb{1}_c - A_4) \mathbb{1}_f - \hat{\mu}_f \mathbb{1}_c) \gamma^0 - \vec{\gamma} \cdot \vec{p} \mathbb{1}_{c,f} - \hat{M}^*(i\omega_k, \vec{p}) \mathbb{1}_d \end{pmatrix}. \quad (42)$$

Using  $\text{Tr} \ln = \ln \det$ , the next step is to calculate the (huge) determinant of this inverse propagator multiplied by  $\beta$ . Using the fact that the determinant of a block diagonal matrix

is the product of the determinants of the blocks, one obtains

$$\begin{aligned}
\det(\beta\tilde{S}^{-1}) &= \det \left\{ \beta \left[ (i\omega_k \mathbb{1}_c - A_4) \mathbb{1}_f + \hat{\mu}_f \mathbb{1}_c \right] \gamma^0 - \vec{\gamma} \cdot \vec{p} \mathbb{1}_{c,f} - \hat{M}(i\omega_k, \vec{p}) \mathbb{1}_d \right\} \cdot \\
&\quad \cdot \det \left\{ \beta \left[ (i\omega_k \mathbb{1}_c - A_4) \mathbb{1}_f - \hat{\mu}_f \mathbb{1}_c \right] \gamma^0 - \vec{\gamma} \cdot \vec{p} \mathbb{1}_{c,f} - \hat{M}^*(i\omega_k, \vec{p}) \mathbb{1}_d \right\} = \\
&= \prod_f \det \left\{ \beta \left[ (i\omega_k \mathbb{1}_c - A_4) + \mu_f \mathbb{1}_c \right] \gamma^0 - \vec{\gamma} \cdot \vec{p} \mathbb{1}_c - \hat{M}(i\omega_k, \vec{p}) \mathbb{1}_d \right\} \cdot \\
&\quad \cdot \det \left\{ \beta \left[ (i\omega_k \mathbb{1}_c - A_4) - \mu_f \mathbb{1}_c \right] \gamma^0 - \vec{\gamma} \cdot \vec{p} \mathbb{1}_c - \hat{M}^*(i\omega_k, \vec{p}) \mathbb{1}_d \right\} = \\
&= \prod_f \det \left\{ \beta \left[ i\omega_{k,f}^- \gamma^0 - \vec{\gamma} \cdot \vec{p} - M(i\omega_k, \vec{p}) \mathbb{1}_d \right] \right\} \det \left\{ \beta \left[ i\omega_{k,f}^{-*} \gamma^0 - \vec{\gamma} \cdot \vec{p} - M^*(i\omega_k, \vec{p}) \mathbb{1}_d \right] \right\} \cdot \\
&\quad \cdot \det \left\{ \beta \left[ i\omega_{k,f}^+ \gamma^0 - \vec{\gamma} \cdot \vec{p} - M(i\omega_k, \vec{p}) \mathbb{1}_d \right] \right\} \det \left\{ \beta \left[ i\omega_{k,f}^{+*} \gamma^0 - \vec{\gamma} \cdot \vec{p} - M^*(i\omega_k, \vec{p}) \mathbb{1}_d \right] \right\} \cdot \\
&\quad \cdot \det \left\{ \beta \left[ i\omega_{k,f}^0 \gamma^0 - \vec{\gamma} \cdot \vec{p} - M(i\omega_k, \vec{p}) \mathbb{1}_d \right] \right\} \det \left\{ \beta \left[ i\omega_{k,f}^{0*} \gamma^0 - \vec{\gamma} \cdot \vec{p} - M^*(i\omega_k, \vec{p}) \mathbb{1}_d \right] \right\} = \\
&= \prod_f \left[ \beta^2 (\omega_{k,f}^-)^2 + \beta^2 \vec{p}^2 + \beta^2 M^2(i\omega_k, \vec{p}) \right]^2 \left[ \beta^2 (\omega_{k,f}^{-*})^2 + \beta^2 \vec{p}^2 + \beta^2 M^{*2}(i\omega_k, \vec{p}) \right]^2 \cdot \\
&\quad \cdot \left[ \beta^2 (\omega_{k,f}^+)^2 + \beta^2 \vec{p}^2 + \beta^2 M^2(i\omega_k, \vec{p}) \right]^2 \left[ \beta^2 (\omega_{k,f}^{+*})^2 + \beta^2 \vec{p}^2 + \beta^2 M^{*2}(i\omega_k, \vec{p}) \right]^2 \cdot \\
&\quad \cdot \left[ \beta^2 (\omega_{k,f}^0)^2 + \beta^2 \vec{p}^2 + \beta^2 M^2(i\omega_k, \vec{p}) \right]^2 \left[ \beta^2 (\omega_{k,f}^{0*})^2 + \beta^2 \vec{p}^2 + \beta^2 M^{*2}(i\omega_k, \vec{p}) \right]^2, \quad (43)
\end{aligned}$$

where the three Matsubara frequencies  $\omega_k^-$ ,  $\omega_k^+$  and  $\omega_k^0$  are the three diagonal components of the colour space matrix  $\hat{\omega}_k := \omega_k \mathbb{1}_c - A_4$  with only diagonal colour matrices taken into account, resulting in  $\omega_k^\pm = \omega_n \pm A_4^3/2 - A_4^8/(2\sqrt{3})$ ,  $\omega_k^0 = \omega_k + A_4^8/\sqrt{3}$ , and the quark chemical potentials are absorbed into the Matsubara frequencies by defining  $\omega_{k,f}^\lambda := \omega_k^\lambda - i\mu_f$ ,  $\lambda = \pm, 0$ .

For the last step we have used that  $\det[\beta(\gamma^0 p^0 - \vec{\gamma} \cdot \vec{p} - m \mathbb{1}_d)] =$

$$= \begin{vmatrix} \beta(p^0 - m) & 0 & -\beta p^3 & -\beta p^1 + i\beta p^2 \\ 0 & \beta(p^0 - m) & -\beta p^1 - i\beta p^2 & \beta p^3 \\ \beta p^3 & \beta p^1 - i\beta p^2 & \beta(-p^0 - m) & 0 \\ \beta p^1 + i\beta p^2 & -\beta p^3 & 0 & \beta(-p^0 - m) \end{vmatrix} = (-\beta^2 p^2 + \beta^2 m^2)^2. \quad (44)$$

Calculating the logarithm of  $\det(\beta\tilde{S}^{-1})$ , one has

$$\begin{aligned}
\Omega &= \frac{\bar{\sigma}^2}{2G} - \frac{1}{\beta} \sum_f \sum_{k=-\infty}^{+\infty} \int \frac{d^3 p}{(2\pi)^3} \times \\
&\quad \times \left[ \ln \left( \beta^2 (\omega_{k,f}^-)^2 + \beta^2 \vec{p}^2 + \beta^2 M^2(i\omega_k, \vec{p}) \right) + \ln \left( \beta^2 (\omega_{k,f}^{-*})^2 + \beta^2 \vec{p}^2 + \beta^2 M^{*2}(i\omega_k, \vec{p}) \right) + \right. \\
&\quad + \ln \left( \beta^2 (\omega_{k,f}^+)^2 + \beta^2 \vec{p}^2 + \beta^2 M^2(i\omega_k, \vec{p}) \right) + \ln \left( \beta^2 (\omega_{k,f}^{+*})^2 + \beta^2 \vec{p}^2 + \beta^2 M^{*2}(i\omega_k, \vec{p}) \right) + \\
&\quad \left. + \ln \left( \beta^2 (\omega_{k,f}^0)^2 + \beta^2 \vec{p}^2 + \beta^2 M^2(i\omega_k, \vec{p}) \right) + \ln \left( \beta^2 (\omega_{k,f}^{0*})^2 + \beta^2 \vec{p}^2 + \beta^2 M^{*2}(i\omega_k, \vec{p}) \right) \right]. \quad (45)
\end{aligned}$$

Taking into account that  $M(i\omega_k, \vec{p}) = \tilde{\mathcal{C}}(i\omega_k, \vec{p})G_S\bar{\sigma}$ , one can perform the variation with respect to  $\bar{\sigma}$  as usual, and in minimising  $\Omega$ , one obtains the mass gap equation

$$1 = \frac{\hat{G}G_S^2}{2\pi^2} \sum_f \sum_{k=-\infty}^{+\infty} \sum_{\lambda=\pm,0} \int_0^\infty \left[ \frac{\tilde{\mathcal{C}}^2(i\hat{\omega}_k, \hat{\rho})\hat{\rho}^2 d\hat{\rho}}{(\hat{\omega}_{k,f}^\lambda)^2 + \hat{\rho}^2 + \hat{\mathcal{C}}^2(i\hat{\omega}_k, \hat{\rho})\hat{\sigma}^2} + \frac{\tilde{\mathcal{C}}^2(i\hat{\omega}_k, \hat{\rho})\hat{\rho}^2 d\hat{\rho}}{(\hat{\omega}_{k,f}^{\lambda*})^2 + \hat{\rho}^2 + \hat{\mathcal{C}}^2(i\hat{\omega}_k, \hat{\rho})\hat{\sigma}^2} \right], \quad (46)$$

where the hatted propagator  $\hat{\mathcal{C}}(i\hat{\omega}_k, \hat{\rho})$  is given by Eq. (38) with all dimensional quantities replaced by dimensionless (hatted) quantities. Note that the right hand side of the mass gap equation that we call the *mass gap function* is real. With  $A_4 = 0$  (no outer field),  $\hat{\omega}_{k,f}^\lambda = \hat{\omega}_k - i\hat{\mu}_f$  does no longer depend on the colour label  $\lambda$ . Therefore, the sum over  $\lambda$  will result in a factor  $N_c$ . One obtains

$$1 = \frac{N_c \hat{G}G_S^2}{\pi^2} \sum_f \sum_{k=-\infty}^{+\infty} \int_0^\infty \frac{(\hat{\omega}_k^2 - \hat{\mu}_f^2 + \hat{\rho}^2 + \hat{\mathcal{C}}^2(i\hat{\omega}_k, \hat{\rho})\hat{\sigma}^2) \hat{\mathcal{C}}^2(i\hat{\omega}_k, \hat{\rho})}{(\hat{\omega}_k^2 - \hat{\mu}_f^2 + \hat{\rho}^2 + \hat{\mathcal{C}}^2(i\hat{\omega}_k, \hat{\rho})\hat{\sigma}^2)^2 + 4\hat{\omega}_k^2 \hat{\mu}_f^2} \hat{\rho}^2 d\hat{\rho}. \quad (47)$$

Taking all quark chemical potentials to be equal, the sum over the flavours  $f$  can be replaced by  $N_f$ . For our standard choice  $N_f = 3$  and  $N_c = 3$  we obtain the solution of the mass gap equation in dependence on  $\hat{\sigma}$  for different values of the reduced chemical potential  $\hat{\mu}_f = \beta\mu_f/2$ . In principle, using the solution of the mass gap equation one can describe the critical temperature in dependence on the chemical potential. In order to see this, one has to get back to dimensional quantities. Depending on  $m_0$  as a constant, the critical temperature can be calculated as  $T_c = m_0/2\hat{m}_0$ . On the other hand, the dimensional quark chemical potential is given by  $\mu_f = 2T_c\hat{\mu}_f$ . Therefore, the abscissa have to be scaled with  $2T_c$ , i.e., the result of the calculation. The best way to show this dependence is via a parametric plot that also suggests that the dependence  $T_c(\mu_f)$  is not a function. Choosing the strong coupling  $\alpha_s$  at the scale of 500 MeV, the parametric plot is shown in Figure 1 for the values  $m_0 = 250$  MeV, 200 MeV, 150 MeV and 116 MeV, the latter close to the expectation.

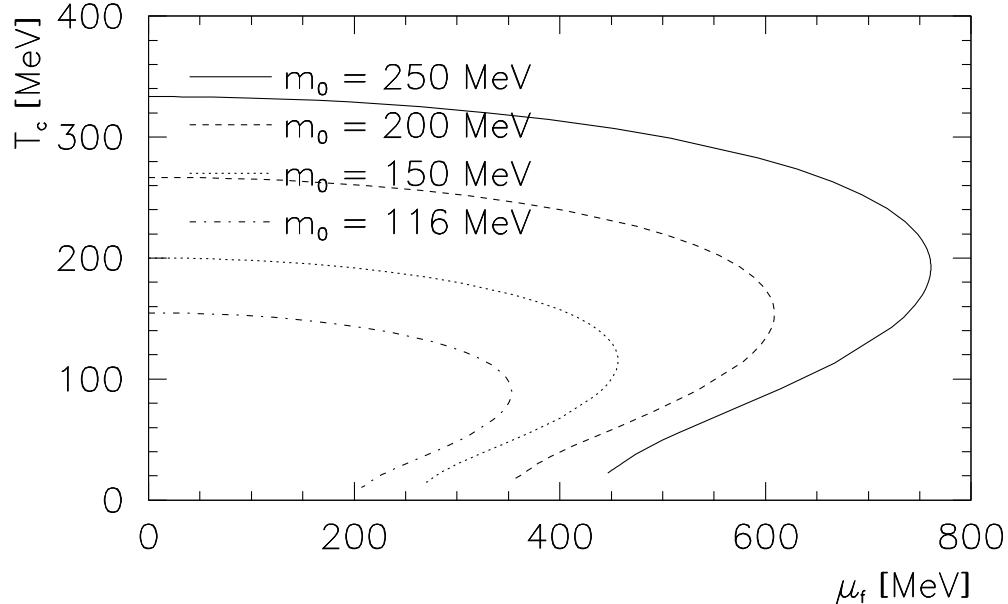


FIG. 1. Dependence of the critical temperature  $T_c$  on the quark chemical potential  $\mu_f$

### C. Adjusting to lattice data

In Ref. [14], a detailed analysis of the critical temperature in dependence on the baryon chemical potential has been performed close to the point  $\mu_B = 0$ . The normalised critical temperature is seen to be an even function of the chemical potential and can be expanded in a Taylor series,<sup>1</sup>

$$\frac{T_c(\mu_B)}{T_c(0)} = 1 - \frac{\kappa_2 \mu_B^2}{T_c(0)^2} - \frac{\kappa_4 \mu_B^4}{T_c(0)^4} + \dots \quad (48)$$

Taking the right hand side of the mass gap equation (47) as a function of  $\hat{\mu}_f^2$  and  $\hat{m}_0^2$ , the mass gap equation  $F(\hat{\mu}_f^2, \hat{m}_0^2) = 1$  can be understood as an implicit equation that related the two variables in a functional way, at least close to  $\mu_B = 0$ . Our first approach to the Taylor coefficients  $\kappa_2$  and  $\kappa_4$  is a numerical one. Approximating the solution of the mass gap equation  $\hat{m}_0^2(\hat{\mu}_f^2)$  in dependence on  $\hat{\mu}_f^2$  by a polynomial up to the power of two in  $\hat{\mu}_f^2$ , one can extract the value  $\hat{m}_0^2$  and the derivatives  $(\hat{m}_0^2)'$  and  $(\hat{m}_0^2)''$  at  $\hat{\mu}_f^2 = 0$ . On the other hand, the functional dependence one aims to determine the Taylor coefficients for is the

<sup>1</sup> The Taylor series expansion shown here is actually given in Ref. [21]. Note that in Ref. [14] the chemical potential was normalised to the critical temperature at the baryon chemical potential, not at the chemical potential at zero. The difference is marginal, though.

one of  $f(\hat{\mu}_f^2) := T_c(\hat{\mu}_f^2)/T_c(0) = \hat{m}_0(0)/\hat{m}_0(\hat{\mu}_f^2)$  on  $g(\hat{\mu}_f^2) := (\mu_B/T_c(0))^2 = (3\mu_f/T_c(0))^2 = 36\hat{\mu}_f^2\hat{m}_0(0)^2/\hat{m}_0(\hat{\mu}_f^2)^2$ . Calculating iteratively

$$\frac{df}{dg} = \frac{f'}{g'}, \quad \frac{d^n f}{dg^n} = \frac{d}{dg} \left( \frac{d^{n-1} f}{dg^{n-1}} \right) = \frac{1}{g'} \left( \frac{d^{n-1} f}{dg^{n-1}} \right), \quad (49)$$

where the prime indicates derivative with respect to  $\hat{\mu}_f^2$ , one can reach up to arbitrary high Taylor coefficients for  $f(g)$ . In this way, we obtain

$$\kappa_2 = \frac{(\hat{m}_0^2)'}{72\hat{m}_0^2}, \quad \kappa_4 = \frac{2(\hat{m}_0^2)''\hat{m}_0^2 + ((\hat{m}_0^2)')^2}{2!(72\hat{m}_0^2)^2}, \quad \dots \quad (50)$$

Having obtained  $\hat{m}_0^2 = 0.374757^2 = 0.140443$ ,  $(\hat{m}_0^2)' = 0.04333$  and  $(\hat{m}_0^2)'' = 0.0055$ , one ends up with  $\kappa_2 = 0.00429$  and  $\kappa_4 = 0.000017$ . These values are roughly one third of the values given in Ref. [14]. However, the choice of the scale of the strong coupling, originally chosen at 500 MeV, can now be used to adjust our prediction to the lattice data. A first sketch unveils that this adjustment is indeed possible. In Fig. 2 we have shown the numerical values for  $\kappa_2$  (upper panel) and  $\kappa_4$  (lower panel) in dependence on the scale of the strong coupling in the interval between 500 and 600 MeV. Shown are also the lattice results including the error bar. It is obvious that close to the right boundary of 600 MeV, there is a chance to match our result to the lattice data.

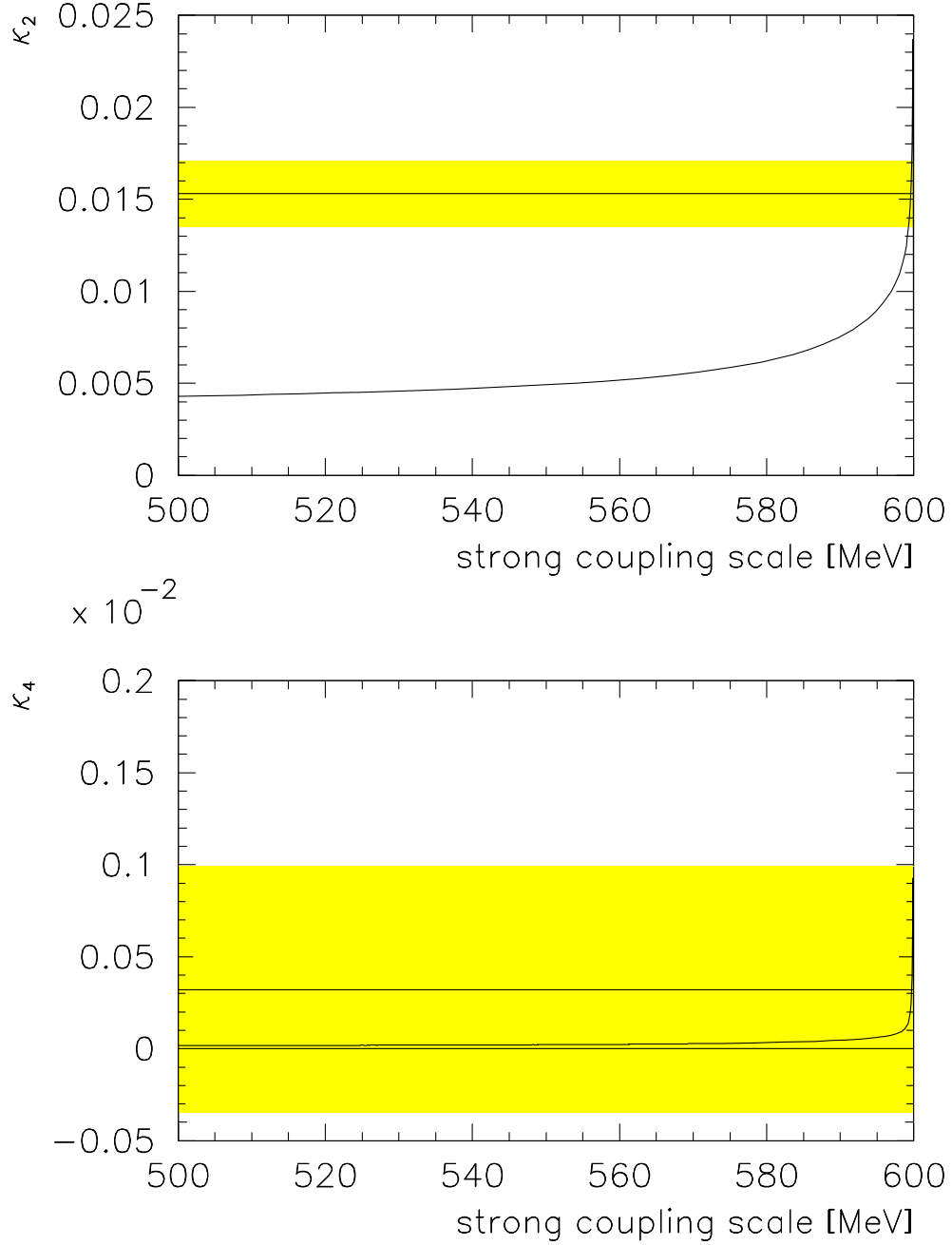


FIG. 2. Values for  $\kappa_2$  (upper panel) and  $\kappa_4$  (lower panel) in dependence on the strong coupling scale, as compared to the values from lattice calculations (yellow band with central line, values taken from Ref. [14])

The matching can be also done semi-analytically. For this we return to the mass gap function  $F(x, y)$  as an implicit function. Taking partial derivatives with respect to the two

arguments  $x = \hat{\mu}_f^2$  and  $y = \hat{m}_0^2$ , we obtain

$$\begin{aligned}
0 &= \frac{\partial F}{\partial x} + \frac{\partial F}{\partial y} \frac{dy}{dx}, \\
0 &= \frac{\partial^2 F}{\partial x^2} + 2 \frac{\partial^2 F}{\partial x \partial y} \frac{dy}{dx} + \frac{\partial^2 F}{\partial y^2} \left( \frac{dy}{dx} \right)^2 + \frac{\partial F}{\partial y} \frac{d^2 y}{dx^2},
\end{aligned} \tag{51}$$

from which we derive

$$\begin{aligned}
\frac{dy}{dx} &= -\frac{\partial F}{\partial x} \left( \frac{\partial F}{\partial y} \right)^{-1}, \\
\frac{d^2 y}{dx^2} &= -\left( \frac{\partial^2 F}{\partial x^2} + 2 \frac{\partial^2 F}{\partial x \partial y} \frac{dy}{dx} + \frac{\partial^2 F}{\partial y^2} \left( \frac{dy}{dx} \right)^2 \right) \left( \frac{\partial F}{\partial y} \right)^{-1} = \\
&= -\left( \frac{\partial^2 F}{\partial x^2} \left( \frac{\partial F}{\partial y} \right)^2 - 2 \frac{\partial^2 F}{\partial x \partial y} \frac{\partial F}{\partial x} \frac{\partial F}{\partial y} + \frac{\partial^2 F}{\partial y^2} \left( \frac{\partial F}{\partial x} \right)^2 \right) \left( \frac{\partial F}{\partial y} \right)^{-3}.
\end{aligned} \tag{52}$$

Via a procedure consisting of different steps that is described for the mass gap function in detail in Appendix B but works in the same way also for the derivatives, one can perform the sum over the Matsubara frequencies explicitly and replace the integration over  $\hat{\rho}$  by a sum over residues. Together with the two-fold sum over the mass states  $m_n = (2n + 1)m_0$

in Eq. (38) of the two propagator factors  $\hat{\mathcal{C}}(\hat{\omega}_k, \hat{\rho})$ , one is left with three-fold summations for

$$\begin{aligned}
F \Big|_{\hat{\mu}_f^2=0} &= -\frac{F_0}{8} \sum_{\nu, \nu_1, \nu_2 \text{ odd}} \frac{2\pi C_{\nu_1}(\kappa) C_{\nu_2}(\kappa)}{\nu_1^2 - \nu_2^2} \times \\
&\quad \times \left( \frac{\sqrt{4\nu_1^2 \hat{m}_0^2 + \nu^2 \pi^2} - |\nu| \pi}{4\nu_1^2 \hat{m}_0^2} - \frac{\sqrt{4\nu_2^2 \hat{m}_0^2 + \nu^2 \pi^2} - |\nu| \pi}{4\nu_2^2 \hat{m}_0^2} \right), \\
\frac{\partial F}{\partial \hat{\mu}_f^2} \Big|_{\hat{\mu}_f^2=0} &= \frac{F_0}{8} \sum_{\nu, \nu_1, \nu_2 \text{ odd}} \frac{8\pi C_{\nu_1}(\kappa) C_{\nu_2}(\kappa)}{\nu_1^2 - \nu_2^2} \times \\
&\quad \times \left( \frac{\sqrt{(4\nu_1^2 \hat{m}_0^2 + \nu^2 \pi^2} - |\nu| \pi)^3}{(4\nu_1^2 \hat{m}_0^2)^3} - \frac{\sqrt{(4\nu_2^2 \hat{m}_0^2 + \nu^2 \pi^2} - |\nu| \pi)^3}{(4\nu_2^2 \hat{m}_0^2)^3} \right), \\
\frac{\partial F}{\partial \hat{m}_0^2} \Big|_{\hat{\mu}_f^2=0} &= \frac{F_0}{8} \sum_{\nu, \nu_1, \nu_2 \text{ odd}} \frac{\pi C_{\nu_1}(\kappa) C_{\nu_2}(\kappa)}{\hat{m}_0^2 (\nu_1^2 - \nu_2^2)} \times \\
&\quad \times \left( \frac{(\sqrt{4\nu_1^2 \hat{m}_0^2 + \nu^2 \pi^2} - |\nu| \pi)^2}{4\nu_1^2 \hat{m}_0^2 \sqrt{4\nu_1^2 \hat{m}_0^2 + \nu^2 \pi^2}} - \frac{(\sqrt{4\nu_2^2 \hat{m}_0^2 + \nu^2 \pi^2} - |\nu| \pi)^2}{4\nu_2^2 \hat{m}_0^2 \sqrt{4\nu_2^2 \hat{m}_0^2 + \nu^2 \pi^2}} \right), \\
\frac{\partial^2 F}{\partial (\hat{\rho}^2)^2} \Big|_{\hat{\mu}_f^2=0} &= -\frac{F_0}{8} \sum_{\nu, \nu_1, \nu_2 \text{ odd}} \frac{64\pi C_{\nu_1}(\kappa) C_{\nu_2}(\kappa)}{\nu_1^2 - \nu_2^2} \times \\
&\quad \times \left( \frac{(\sqrt{4\nu_1^2 \hat{m}_0^2 + \nu^2 \pi^2} - |\nu| \pi)^5}{(4\nu_1^2 \hat{m}_0^2)^5} - \frac{(\sqrt{4\nu_2^2 \hat{m}_0^2 + \nu^2 \pi^2} - |\nu| \pi)^5}{(4\nu_2^2 \hat{m}_0^2)^5} \right), \\
\frac{\partial^2 F}{\partial \hat{\rho}^2 \partial \hat{m}_0^2} \Big|_{\hat{\mu}_f^2=0} &= -\frac{F_0}{8} \sum_{\nu, \nu_1, \nu_2 \text{ odd}} \frac{12\pi C_{\nu_1}(\kappa) C_{\nu_2}(\kappa)}{\hat{m}_0^2 (\nu_1^2 - \nu_2^2)} \times \\
&\quad \times \left( \frac{(\sqrt{4\nu_1^2 \hat{m}_0^2 + \nu^2 \pi^2} - |\nu| \pi)^4}{(4\nu_1^2 \hat{m}_0^2)^3 \sqrt{4\nu_1^2 \hat{m}_0^2 + \nu^2 \pi^2}} - \frac{(\sqrt{4\nu_2^2 \hat{m}_0^2 + \nu^2 \pi^2} - |\nu| \pi)^4}{(4\nu_2^2 \hat{m}_0^2)^3 \sqrt{4\nu_2^2 \hat{m}_0^2 + \nu^2 \pi^2}} \right), \\
\frac{\partial^2 F}{\partial (\hat{m}_0^2)^2} \Big|_{\hat{\mu}_f^2=0} &= -\frac{F_0}{8} \sum_{\nu, \nu_1, \nu_2 \text{ odd}} \frac{\pi C_{\nu_1}(\kappa) C_{\nu_2}(\kappa)}{2\hat{m}_0^4 (\nu_1^2 - \nu_2^2)} \times \\
&\quad \times \left( \frac{(\sqrt{4\nu_1^2 \hat{m}_0^2 + \nu^2 \pi^2} - |\nu| \pi)^3 (3\sqrt{4\nu_1^2 \hat{m}_0^2 + \nu^2 \pi^2} + |\nu| \pi)}{4\nu_1^2 \hat{m}_0^2 (4\nu_1^2 \hat{m}_0^2 + \nu^2 \pi^2)^{3/2}} + \right. \\
&\quad \left. - \frac{(\sqrt{4\nu_2^2 \hat{m}_0^2 + \nu^2 \pi^2} - |\nu| \pi)^3 (3\sqrt{4\nu_2^2 \hat{m}_0^2 + \nu^2 \pi^2} + |\nu| \pi)}{4\nu_2^2 \hat{m}_0^2 (4\nu_2^2 \hat{m}_0^2 + \nu^2 \pi^2)^{3/2}} \right). \tag{53}
\end{aligned}$$

In order to begin with the numerical analysis and to match the lattice results, we start with the value of the general factor  $F_0$  that contains the strong coupling, for  $\kappa = -1$  given by

$$F_0 = \frac{N_f N_c \hat{G} G_S^2}{\pi^2} = 3 \times 3 \times \frac{K(-1)^2}{\pi^2} \times \frac{16\pi \alpha_s}{9\pi^2} = \frac{16}{\pi^3} K(-1)^2 \alpha_s = 0.886941 \alpha_s. \tag{54}$$

The Taylor coefficient  $\hat{m}_0(\hat{\mu}_f^2 = 0)$  is solution of  $F(0, \hat{m}_0^2) = 1$ . The dependence of  $F(0, \hat{m}_0)$

shows a saturation for high values of  $\hat{m}_0$  at approximately  $0.28F_0 = 0.25\alpha_s$ . Therefore, in order that the mass gap equation is satisfied,  $\alpha_s$  has to be larger than 4.0. In our case at the perturbative scale of 500 MeV, we have  $\hat{m}_0 = 0.374757$ . Inserting this value into the derivatives and using these to calculate the slope and the curvature of  $\hat{m}_0^2(\hat{\mu}_f^2)$  according to Eq. (52), one obtains

$$(\hat{m}_0^2)' = \left. \frac{d(\hat{m}_0^2)}{d(\hat{\mu}_f^2)} \right|_{\hat{\mu}_f^2=0} = 0.0433332, \quad (\hat{m}_0^2)'' = \left. \frac{d^2(\hat{m}_0^2)}{d(\hat{\mu}_f^2)^2} \right|_{\hat{\mu}_f^2=0} = 0.0110326, \quad (55)$$

that are in nice agreement with the previous numerical values, or improve their precision (note that the calculation of the second derivative very much depends on the mesh length of the approximation). The resulting coefficients are given by  $\kappa_2 = 0.00429$  and  $\kappa_4 = 0.000024$ . In order to adjust to the lattice values  $\kappa_2 = 0.0153(18)$  and  $\kappa_4 = 0.00032(67)$  found in Ref. [14], we have to solve  $(\hat{m}_0^2)' = 72\hat{m}_0^2\kappa_2$ , or

$$\frac{\partial F}{\partial \hat{\mu}_f^2} + 72\kappa_2\hat{m}_0^2 \frac{\partial F}{\partial \hat{m}_0^2} = 0, \quad (56)$$

which is an implicit equation for  $\hat{m}_0$ . For  $\kappa_2 = 0.0153$ , the matching procedure gives  $\hat{m}_0 = 7.7503$ . For this value, one has  $F(0, \hat{m}_0^2) = 0.278128F_0$  and  $\kappa_4 = 0.000314$ . The value of the coupling corresponding to this is  $\alpha_s = 4.05379$ .

#### IV. DISCUSSION AND CONCLUSIONS

Using a closed-form solution for the correlation functions of the Yang–Mills theory, we show how to derive a non-local Nambu–Jona-Lasinio model directly from QCD, describing the behaviour of the theory away from the asymptotic freedom regime. This model has also been proven to be confining [55] and to be able to give results for the hadron vacuum polarisation correction to the muon’s  $g - 2$  factor in agreement with the experiment [39]. In this work, we extend the applicability of this model in regimes of finite temperature and chemical potential where lattice data are available. We were able to show that:

- The theory displays a phase transition in agreement with the lattice data results, yielding the crossover point of the chiral phase transition.

- We derive the critical temperature  $T_c$  as a function of the chemical potential  $\mu_f$  in Eq. (47). In Fig. 1, we show such a dependence at varying a single parameter representing the proper scale of the model (the QCD scale  $m_0$ ). This parameter arises from the integration of the Yang-Mills theory, determines the spectrum of the theory, and yields the mass gap. We are able to obtain an excellent agreement with lattice data related to the physical scale we are ranging on.
- We evaluate the coefficients  $\kappa_2$  and  $\kappa_4$  of the Taylor expansion of  $T_c(\mu_B)$  around  $\mu_B = 0$  and find agreement with lattice data in a large range of values of our QCD scale  $m_0$  common to both coefficients. This is shown in Fig. 2 where the yellow bands show the agreement zone with lattice data as a function of  $m_0$ .

We aim to obtain the QCD equation of state in our future works. Due to the possible dynamics coming from the quark–gluon plasma and the electroweak transitions, they impact the propagation of primordial gravitational waves (PGWs) in the early universe [56–58], with prospects for measurements in current and upcoming gravitational wave (GW) experiments like DECIGO [59, 60], LISA [61], SKA [62], and EPTA [63] across various frequency ranges with quantified estimates shown in Ref. [64]. The results obtained will have large impact for the understanding of such GW measurements. Besides this, we envisage also to have applications of our results in precise estimates of relic density of dark matter in the early universe and its experimental direct detection [65, 66], and cosmological phase transition with observable effects [67, 68]. For detailed analyses on these topics see Refs. [56, 65, 67, 69–76]. In particular, the effect of considering finite non-zero chemical potential, as it is studied in this paper, may modify the strength of the cosmological transition with inevitable consequences for the early universe if it undergoes a first or second order phase transition [77, 78]. This may also lead to a difference in the equation of state when compared to the case of zero chemical potentials [72, 79]. Such cosmological analyses are beyond the scope of the current paper and we leave these to future work.

## Appendix A: On the normalised two-point Green function $\mathcal{C}(x)$

The normalised two-point Green function is given by  $\mathcal{C}(z) = 2iG_2(x)/G$ , where  $G$  is obtained in turn by calculating  $\tilde{G}_2(0) = \int G_2(z)d^4z = -iG/2$ . This is easy to do. Indeed, on the one hand one has

$$\text{sn}(\zeta|\kappa) = \frac{2\pi}{K(\kappa)\sqrt{\kappa}} \sum_{n=0}^{\infty} \frac{q^{n+1/2}}{1-q^{2n+1}} \sin\left((2n+1)\frac{\pi\zeta}{2K(\kappa)}\right), \quad (\text{A1})$$

and for  $\zeta = K(\kappa)$

$$1 = \text{sn}(K(\kappa)|\kappa) = \frac{2\pi}{K(\kappa)} \sum_{n=0}^{\infty} \frac{q^{n+1/2}}{\sqrt{\kappa}(1-q^{2n+1})} \sin\left((2n+1)\frac{\pi}{2}\right) = \frac{2\pi}{K(\kappa)} \sum_{n=0}^{\infty} \frac{(-1)^n q^{n+1/2}}{\sqrt{\kappa}(1-q^{2n+1})}. \quad (\text{A2})$$

On the other hand,

$$\tilde{G}_2(0) = \sum_{n=0}^{\infty} \frac{iB_n}{-m_n^2} = \frac{-2\pi i}{(1-\kappa)K(\kappa)k^2} \sum_{n=0}^{\infty} \frac{(-1)^n q^{n+1/2}}{\sqrt{\kappa}(1-q^{2n+1})} = \frac{-i}{(1-\kappa)k^2} = -\frac{iG}{2}. \quad (\text{A3})$$

Therefore, one has  $G = 2/((1-\kappa)k^2)$ .

## Appendix B: The mass gap function and its derivatives

Starting point is the mass gap function

$$F(\hat{\mu}_f^2, \hat{m}_0^2) = \frac{F_0}{\hat{m}_0^2} \sum_{k=-\infty}^{+\infty} \int_0^{\infty} \frac{(\hat{\omega}_k^2 + \hat{\rho}^2 - \hat{\mu}_f^2) \tilde{\mathcal{C}}^2(i\hat{\omega}_k, \hat{\rho})}{(\hat{\omega}_k^2 + \hat{\rho}^2 - \hat{\mu}_f^2)^2 + 4\hat{\omega}_k^2 \hat{\mu}_f^2} \hat{\rho}^2 d\hat{\rho} =: F(\hat{\mu}_f^2, \hat{m}_0^2) \quad (\text{B1})$$

with  $F_0 := N_c N_f \hat{G} G_S^2 / \pi^2$ . The first step is the introduction of Feynman parameters, according to

$$\frac{1}{A_1^{\alpha_1} \dots A_m^{\alpha_m}} = \frac{\Gamma(\alpha_1 + \dots + \alpha_m)}{\Gamma(\alpha_1) \dots \Gamma(\alpha_m)} \int_0^1 \frac{x_1^{\alpha_1-1} \dots x_m^{\alpha_m-1} \delta(x_1 + \dots + x_m - 1)}{(x_1 A_1 + \dots + x_m A_m)^{\alpha_1 + \dots + \alpha_m}} dx_1 \dots dx_m, \quad (\text{B2})$$

while the second step is the explicit summation over the Matsubara frequencies,

$$\begin{aligned} F(\hat{\mu}_f^2, \hat{m}_0^2) &= F_0 \sum_{k=-\infty}^{+\infty} \sum_{n_1, n_2=0}^{\infty} \int_0^{\infty} \frac{\hat{m}_0^2 C_{2n_1+1}(\kappa) C_{2n_2+1}(\kappa) \hat{\rho}^2 d\hat{\rho}}{(\hat{\omega}_k^2 + \hat{\rho}^2 + (2n_1+1)^2 \hat{m}_0^2)(\hat{\omega}_k^2 + \hat{\rho}^2 + (2n_2+1)^2 \hat{m}_0^2)(\hat{\omega}_k^2 + \hat{\rho}^2)} = \\ &= F_0 \sum_{k=-\infty}^{+\infty} \sum_{n_1, n_2=0}^{\infty} \int_0^{\infty} \int_0^1 dx_1 \int_0^{1-x_1} dx_2 \frac{\Gamma(3) C_{2n_1+1}(\kappa) C_{2n_2+1}(\kappa) \hat{m}_0^2 \hat{\rho}^2 d\hat{\rho}}{(\hat{\omega}_k^2 + \hat{\rho}^2 + x_1(2n_1+1)^2 \hat{m}_0^2 + x_2(2n_2+1)^2 \hat{m}_0^2)^3} = \\ &= F_0 \sum_{n_1, n_2=0}^{\infty} C_{2n_1+1}(\kappa) C_{2n_2+1}(\kappa) \int_0^1 dx_1 \int_0^{1-x_1} dx_2 \times \\ &\quad \times \int_0^{\infty} \frac{\hat{m}_0^2 \hat{\rho}^2 d\hat{\rho}}{4\hat{a}^5} \left[ 2\hat{a}^2 \tanh^3 \hat{a} + 3\hat{a} \tanh^2 \hat{a} + (3-2\hat{a}^2) \tanh \hat{a} - 3\hat{a} \right] \end{aligned} \quad (\text{B3})$$

with  $\hat{a}^2 = \hat{\rho}^2 + \hat{m}^2$  and  $\hat{m}^2 = x_1(2n_1 + 1)^2\hat{m}_0^2 + x_2(2n_2 + 1)^2\hat{m}_0^2$ . Applying Cauchy's residue theorem, the integrand provides poles up to degree 5 at  $\hat{\rho} = \pm i\hat{m}$  from the general factor and poles up to degree 3 at  $\hat{\rho} = \pm i\sqrt{\hat{m}^2 + (2n + 1)^2\pi^2/4}$  from the hyperbolic tangent functions. While the former residues related to the first poles vanish, the residues of the latter are given by

$$\frac{\mp 2i}{(4\hat{m}^2 + (2n + 1)^2\pi^2)^{3/2}}. \quad (\text{B4})$$

One obtains

$$F(\hat{\mu}_f^2, \hat{m}_0^2) = F_0 \sum_{n, n_1, n_2=0}^{\infty} \int_0^1 dx_1 \int_0^{1-x_1} dx_2 \times \frac{2\pi C_{2n_1+1}(\kappa) C_{2n_2+1}(\kappa) \hat{m}_0^2}{(4x_1(2n_1 + 1)^2\hat{m}_0^2 + 4x_2(2n_2 + 1)^2\hat{m}_0^2 + (2n + 1)^2\pi^2)^{3/2}}. \quad (\text{B5})$$

Finally, the integrations over the Feynman parameters  $x_1$  and  $x_2$  can be performed to give

$$F(\hat{\mu}_f^2, \hat{m}_0^2) = \frac{F_0}{8} \sum_{\nu, \nu_1, \nu_2 \text{ odd}} \frac{2\pi C_{\nu_1}(\kappa) C_{\nu_2}(\kappa)}{\nu_1^2 - \nu_2^2} \times \left( \frac{\sqrt{4\nu_2^2\hat{m}_0^2 + \nu^2\pi^2} - |\nu|\pi}{4\nu_2^2\hat{m}_0^2} - \frac{\sqrt{4\nu_1^2\hat{m}_0^2 + \nu^2\pi^2} - |\nu|\pi}{4\nu_1^2\hat{m}_0^2} \right). \quad (\text{B6})$$

In this expression we have used  $\nu = 2n + 1$ ,  $\nu_1 = 2n_1 + 1$  and  $\nu_2 = 2n_2 + 1$  and symmetrised the summation, giving rise to the factor 1/8. The partial derivatives of this mass gap function are handled in the same way. Note that in calculating  $\kappa_2$  and  $\kappa_4$ , the general factor  $F_0$  cancels out. Only the original mass gap equation depends in the value of  $F_0$ .

- 
- [1] M. Arslanok *et al.* [arXiv:2303.17254 [nucl-ex]].
  - [2] X. An *et al.* Nucl. Phys. A **1017**, 122343 (2022).
  - [3] J. H. Putschke *et al.* [arXiv:1903.07706 [nucl-th]].
  - [4] D. R. Phillips *et al.* J. Phys. G **48**, no.7, 072001 (2021).
  - [5] Z. Fodor, S. D. Katz, JHEP **0203**, 014 (2002).
  - [6] Y. Aoki, G. Endrodi, Z. Fodor, S. D. Katz, K. K. Szabo, Nature **443**, 675-678 (2006).
  - [7] Y. Aoki, S. Borsanyi, S. Durr, Z. Fodor, S. D. Katz, S. Krieg and K. K. Szabo, JHEP **0906**, 088 (2009).

- [8] A. Bazavov *et al.*, Phys. Rev. D **80**, 014504 (2009).
- [9] P. de Forcrand, PoS **LAT2009**, 010 (2009).
- [10] S. Borsanyi, G. Endrodi, Z. Fodor, S. D. Katz, S. Krieg, C. Ratti and K. K. Szabo, JHEP **08**, 053 (2012).
- [11] A. Bazavov, H. T. Ding, P. Hegde, O. Kaczmarek, F. Karsch, E. Laermann, Y. Maezawa, S. Mukherjee, H. Ohno and P. Petreczky, *et al.* Phys. Rev. D **95**, no.5, 054504 (2017).
- [12] C. Bonati, M. D’Elia, F. Negro, F. Sanfilippo and K. Zambello, Phys. Rev. D **98**, no.5, 054510 (2018).
- [13] A. Bazavov *et al.* [HotQCD], Phys. Lett. B **795**, 15-21 (2019).
- [14] S. Borsanyi, Z. Fodor, J. N. Guenther, R. Kara, S. D. Katz, P. Parotto, A. Pasztor, C. Ratti and K. K. Szabo, Phys. Rev. Lett. **125**, no.5, 052001 (2020).
- [15] S. Borsányi, Z. Fodor, J. N. Guenther, R. Kara, S. D. Katz, P. Parotto, A. Pásztor, C. Ratti and K. K. Szabó, Phys. Rev. Lett. **126**, no.23, 232001 (2021).
- [16] M. Kahangirwe, S. A. Bass, E. Bratkovskaya, J. Jahan, P. Moreau, P. Parotto, D. Price, C. Ratti, O. Soloveva and M. Stephanov, Phys. Rev. D **109**, no.9, 094046 (2024).
- [17] K. Splittorff and J. J. M. Verbaarschot, Phys. Rev. D **75**, 116003 (2007).
- [18] S. D. H. Hsu and D. Reeb, Int. J. Mod. Phys. A **25**, 53-67 (2010).
- [19] G. Aarts, PoS **LATTICE2012**, 017 (2012).
- [20] K. Nagata, Prog. Part. Nucl. Phys. **127**, 103991 (2022).
- [21] Y. Lu, F. Gao, Y. X. Liu and J. M. Pawłowski, Phys. Rev. D **110**, no.1, 014036 (2024).
- [22] S. Borsanyi *et al.* [Wuppertal-Budapest], JHEP **09**, 073 (2010).
- [23] A. Bazavov *et al.* Phys. Rev. D **85**, 054503 (2012).
- [24] T. Bhattacharya *et al.* Phys. Rev. Lett. **113**, no.8, 082001 (2014).
- [25] A. Bazavov *et al.* [HotQCD], Phys. Rev. D **90**, 094503 (2014).
- [26] K. Fukushima, Phys. Lett. B **591**, 277-284 (2004).
- [27] E. Megias, E. Ruiz Arriola and L. L. Salcedo, Phys. Rev. D **74**, 065005 (2006).
- [28] C. Ratti, M. A. Thaler and W. Weise, Phys. Rev. D **73**, 014019 (2006).
- [29] B. J. Schaefer, J. M. Pawłowski and J. Wambach, Phys. Rev. D **76**, 074023 (2007).
- [30] V. Skokov, B. Stokic, B. Friman and K. Redlich, Phys. Rev. C **82**, 015206 (2010).

- [31] T. K. Herbst, J. M. Pawłowski and B. J. Schaefer, Phys. Lett. B **696**, 58-67 (2011).
- [32] M. Drews and W. Weise, Prog. Part. Nucl. Phys. **93**, 69-107 (2017).
- [33] K. Fukushima and V. Skokov, Prog. Part. Nucl. Phys. **96**, 154-199 (2017).
- [34] C. D. Roberts and S. M. Schmidt, Prog. Part. Nucl. Phys. **45**, S1-S103 (2000).
- [35] C. S. Fischer, Prog. Part. Nucl. Phys. **105**, 1-60 (2019).
- [36] M. Frasca, Eur. Phys. J. Plus **132**, no.1, 38 (2017) [erratum: Eur. Phys. J. Plus **132**, no.5, 242 (2017)].
- [37] S. Fubini, Nuovo Cim. A **34**, 521 (1976).
- [38] L. N. Lipatov, Sov. Phys. JETP **45**, 216-223 (1977). LENINGRAD-76-255.
- [39] M. Frasca, A. Ghoshal and S. Groote, Phys. Rev. D **104**, no.11, 114036 (2021).
- [40] A. Boccaletti, S. Borsanyi, M. Davier, Z. Fodor, F. Frech, A. Gerardin, D. Giusti, A. Y. Kotov, L. Lellouch and T. Lippert, *et al.* [arXiv:2407.10913 [hep-lat]].
- [41] A. Bazavov *et al.* [Fermilab Lattice, HPQCD and MILC], [arXiv:2411.09656 [hep-lat]].
- [42] D. P. Aguillard *et al.* [Muon g-2], Phys. Rev. Lett. **131**, no.16, 161802 (2023).
- [43] D. P. Aguillard *et al.* [Muon g-2], Phys. Rev. D **110**, no.3, 032009 (2024).
- [44] M. Frasca, Int. J. Mod. Phys. E **18**, 693 (2009).
- [45] M. Frasca, Phys. Rev. C **84**, 055208 (2011).
- [46] M. Frasca, AIP Conf. Proc. **1492**, 177 (2012).
- [47] M. Frasca, Nucl. Phys. Proc. Suppl. **234**, 329 (2013).
- [48] M. Frasca, J. Nonlin. Math. Phys. **18**, 291 (2011).
- [49] M. Frasca, Mod. Phys. Lett. **A24**, 2425-2432 (2009).
- [50] M. Frasca, Phys. Lett. B **670**, 73 (2008).
- [51] U. Vogl and W. Weise, Prog. Part. Nucl. Phys. **27**, 195-272 (1991).
- [52] S. P. Klevansky, Rev. Mod. Phys. **64**, 649-708 (1992).
- [53] Michael Buballa, Phys. Rept. **407**, 205-376 (2005).
- [54] T. Hell, S. Rößner, M. Cristoforetti and W. Weise, Phys. Rev. D **79**, 014022 (2009).
- [55] M. Frasca, A. Ghoshal and S. Groote, Phys. Lett. B **846**, 138209 (2023).
- [56] D. J. Schwarz, Mod. Phys. Lett. A **13**, 2771-2778 (1998).
- [57] M. Maggiore, Phys. Rept. **331**, 283-367 (2000).

- [58] A. Mazumdar and G. White, Rept. Prog. Phys. **82**, no.7, 076901 (2019).
- [59] N. Seto, S. Kawamura and T. Nakamura, Phys. Rev. Lett. **87**, 221103 (2001).
- [60] S. Sato *et al.* J. Phys. Conf. Ser. **840**, no.1, 012010 (2017).
- [61] P. Amaro-Seoane *et al.* [LISA], [arXiv:1702.00786 [astro-ph.IM]].
- [62] G. Janssen *et al.* PoS **AASKA14**, 037 (2015).
- [63] L. Lentati *et al.* [EPTA], Mon. Not. Roy. Astron. Soc. **453**, no.3, 2576-2598 (2015).
- [64] F. Hajkarim, J. Schaffner-Bielich, S. Wüstebach and M. M. Wygas, Phys. Rev. D **99**, no.10, 103527 (2019).
- [65] M. Drees, F. Hajkarim and E. R. Schmitz, JCAP **06**, 025 (2015).
- [66] G. Steigman, B. Dasgupta and J. F. Beacom, Phys. Rev. D **86**, 023506 (2012).
- [67] S. Capozziello, M. Khodadi and G. Lambiase, Phys. Lett. B **789**, 626-633 (2019).
- [68] M. Khodadi, U. K. Dey and G. Lambiase, Phys. Rev. D **104**, no.6, 063039 (2021).
- [69] P. Castorina, D. Lanteri and S. Mancani, Phys. Rev. D **98**, no.2, 023007 (2018).
- [70] S. Anand, U. K. Dey and S. Mohanty, JCAP **03**, 018 (2017).
- [71] D. J. Schwarz, Annalen Phys. **12**, 220-270 (2003).
- [72] M. Stuke, D. J. Schwarz and G. Starkman, JCAP **03**, 040 (2012).
- [73] K. Saikawa and S. Shirai, JCAP **05**, 035 (2018).
- [74] M. Hindmarsh and O. Philipsen, Phys. Rev. D **71**, 087302 (2005).
- [75] S. Borsanyi *et al.* Nature **539**, no.7627, 69-71 (2016).
- [76] M. W. Li, Y. Yang and P. H. Yuan, [arXiv:1812.09676 [hep-th]].
- [77] E. Witten, Phys. Rev. D **30**, 272-285 (1984).
- [78] M. Asakawa and K. Yazaki, Nucl. Phys. A **504**, 668-684 (1989).
- [79] D. J. Schwarz and M. Stuke, JCAP **11**, 025 (2009) [erratum: JCAP **10**, E01 (2010)].